Available online at www.sciencedirect.com
SCIENCE DIRECT®
Physica D 199 (2004) 91–104
PHYSICA D
www.elsevier.com/locate/physd

Spectral properties and pattern selection in fractal growth networks

K. Tucci[a,b,*], M.G. Cosenza[c]

[a] *Max-Planck-Institut für Physik Komplexer Systeme, Nöthnizer Strasse 38, 01187 Dresden, Germany*
[b] *SUMA-CeSiMo, Universidad de Los Andes, Mérida 5251, Venezuela*
[c] *Facultad de Ciencias, Centro de Astrofísica Teorica, Universidad de Los Andes, Apartado Postal 26 La Hechicera, Mérida 5251, Venezuela*

Abstract

A model for the generation of fractal growth networks in Euclidean spaces of arbitrary dimension is presented. These networks are considered as the spatial support of reaction–diffusion and pattern formation processes. The local dynamics at the nodes of a fractal growth network is given by a nonlinear map, giving raise to a coupled map system. The coupling is described by a matrix whose eigenvectors constitute a basis on which spatial patterns on fractal growth networks can be expressed by linear combination. The spectrum of eigenvalues the coupling matrix exhibits a nonuniform distribution that is reflected in the presence of gaps or niches in the boundaries of stability of the synchronized states on the space of parameters of the system. These gaps allow for the selection of specific spatial patterns by appropriately varying the parameters of the system.

PACS: 05.45.−a; 02.50.−r

Keywords: Pattern formation; Fractal networks; Coupled map systems; Synchronization

1. Introduction

Pattern formation processes in regimes far from equilibrium often take place on media that are nonuniform at some length scales. The nonuniformity may be due to the intrinsic heterogeneous nature of the substratum, typical of pattern formation in biological contexts, or it may arise from random imperfections or fluctuations in the medium. Such heterogeneities can have significant effects on the form of spatial patterns, for example, they can induce reberverators in excitable media and defects can serve as nucleation sites for domain growth processes.

* Corresponding author.
E-mail address: kay@ula.ve (K. Tucci).

0167-2789/$ – see front matter © 2004 Elsevier B.V. All rights reserved.
doi:10.1016/j.physd.2004.08.005

Recently, there has been much interest in the study of spatiotemporal dynamical processes on nonuniform or complex networks. In this context, coupled map lattices [1] have provided fruitful and computationally efficient models for the investigation of a variety of dynamical processes in spatially distributed systems. In particular, the discrete-space character of coupled map systems makes them specially appropriate for the investigation of spatiotemporal dynamics on nonuniform networks that can represent models of heterogeneous media. Phenomena such as pattern formation, spatiotemporal intermittency, nontrivial collective behavior, synchronization, phase-ordering, etc., have been extensively studied in coupled map systems defined on fractal lattices [2,3], hierarchical structures [4], trees [5], random graphs [6], small-world networks [7], and scale-free networks [8].

An especially interesting class of nonuniform geometries comprises fractal growth networks [9] whose branching structure, self-similar scaling features and lack of translation symmetry can give rise to several distinct characteristics in both their dynamical and spatial properties. Fractal growth structures appear in nonequilibrium growth processes which are common in many areas. Examples of such phenomena include diffusion-limited aggregation, dendritic solidification, bacterial growth, viscous fingering, capillarity, electrodeposition, Laplacian growth problems, etc. [10].

In this article we consider discrete reaction–diffusion processes and pattern formation taking place on fractal growth networks. The spatiotemporal dynamics corresponds to a coupled map system defined on the geometrical support of a fractal growth network. Although many growth structures found in nature have random features, here we study the case of simple, deterministic fractal growth networks. We focus on the changes occurred in spatiotemporal patterns as a result of the fractal growth connectivity that describes the interactions in the system. In Section 2, a model for the construction of fractal growth networks in any Euclidean space and a general notation for their treatment are introduced. In Section 3, the coupled map models defined on fractal growth networks are presented. The diffusion coupling among neighboring sites on a network is described by a matrix. The spectrum of eigenvalues and eigenvectors of the coupling matrix is analyzed in Section 4. The eigenvectors constitute a complete basis on which spatial patterns can be expressed by a linear combination. Section 5 contains a study of the stability of spatially uniform, periodic patterns on a fractal growth network for a local dynamics given by the logistic map. Distinct features, emerging as a consequence of the fractal nature of the networks, allow for the selection of specific spatial patterns as the parameters of the system are changed. Conclusions are presented in Section 6.

2. Model for fractal growth networks

Fractal growth networks can be generated in any Euclidean space of dimension d by generalizing the fractal growth model of Vicsek [9]. Starting from a d-dimensional hypercube, it is divided into 3^d equal hypercubes. Of these, only the central hypercube plus the 2^d hypercubes connected to its vertices are kept. This process is repeated for each of the $2^d + 1$ resulting hypercubes. At a level of construction L, the network consists of $N = (2^d + 1)^L$ hypercubical cells or nodes whose coordinates can be specified by a sequence of symbols $(\alpha_1\alpha_2 \cdots \alpha_L)$, where α_i can take any value in a collection of $2^d + 1$ different digits forming an enumeration system in base $(2^d + 1)$, which we denote by $\{\epsilon_1, \epsilon_2, \ldots, \epsilon_{2^{d+1}+1}\}$. For example, for $d = 2$, we may chose $\alpha_i \in \{0, 1, 2, 3, 4\}$.

To fix the labels, we start at level $L = 1$ where the labels of the $2^d + 1$ cells in the network have the form (α_1). The label (0) is assigned to the central cell, and the others 2^d cells are labeled by $(\alpha_i) \neq (0)$ in such a way that the labels (α_i) and (α_j) of the two cells located at the opposite ends of each diagonal passing through the central cell satisfy $\mathrm{mod}_{2^d+1}(\alpha_i + \alpha_j) = 0$, where the addition $\alpha_i + \alpha_j$ is defined modulo $(2^d + 1)$. Fig. 1(a) and (b) show this notation for the fractal growth networks embedded in Euclidean spaces of dimension $d = 2$ and 3, respectively.

When the fractal network grows from level of construction L to level $(L + 1)$, each cell $(\alpha_1\alpha_2 \cdots \alpha_L)$ is subdivided into $2^d + 1$ cells, scaled down by a longitudinal factor of 3, and which are now labeled by $(\alpha_1\alpha_2 \cdots \alpha_L\alpha_{L+1})$, where the first L symbols of the sequence, $\alpha_1\alpha_2 \cdots \alpha_L$, are the same as in the parent cell, and to distinguish the $(2^d + 1)$

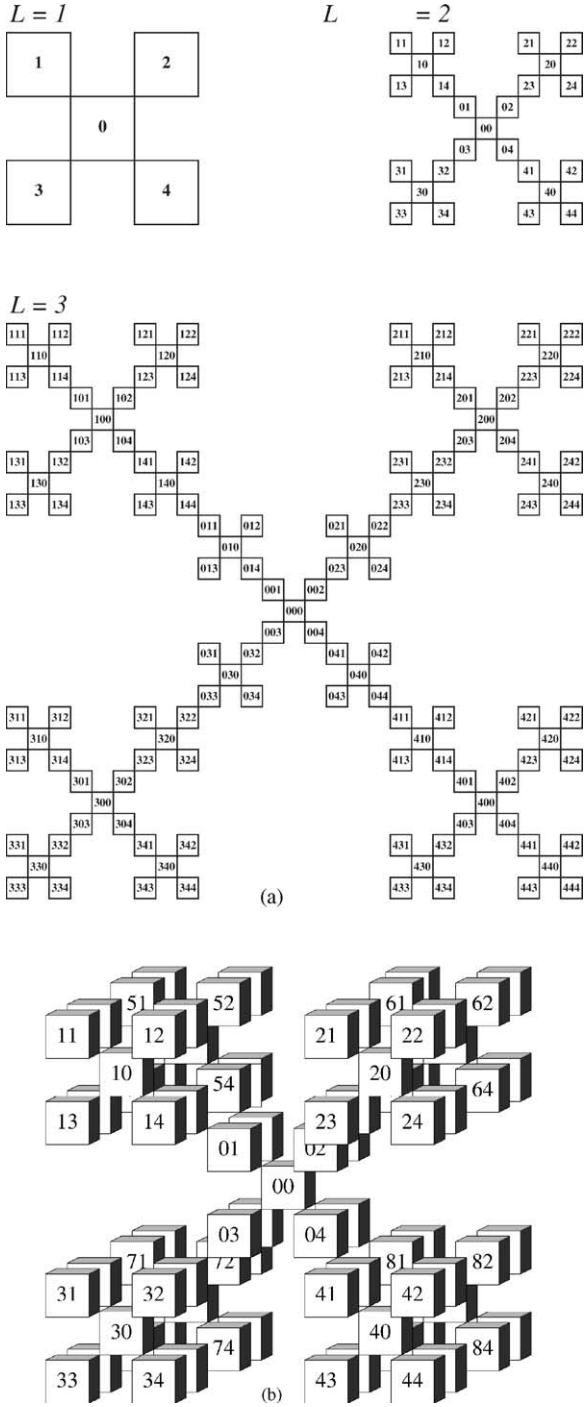

Fig. 1. (a) Fractal growth network embedded in Euclidean space of dimension $d = 2$ at levels of construction $L = 1$, 2 and 3, showing labels on the cells. (b) Fractal growth network embedded in dimension $d = 3$ at level of construction $L = 2$, showing labels on the cells.

daughter cells, the last symbol α_{L+1} is assigned similarly to the labels (α_1) at the construction level $L = 1$. From the construction process, it follows that the fractal dimension of the network is $d_f = \ln(2^d + 1)/\ln 3$.

The set of cells connected to the cell labeled by $(\alpha_1\alpha_2\cdots\alpha_L)$ at a level of construction L is defined as the neighborhood (nearest neighbors) of this cell, and will be denoted by $\mathcal{N}(\alpha_1\alpha_2\cdots\alpha_L)$. Three types of cells can be identified in a fractal growth network embedded in a d-dimensional Euclidean space: (i) centers, that are connected to 2^d other cells; (ii) joints, that are connected to two cells; (iii) edges, connected to just one cell. A sequence $(\alpha_1\alpha_2\cdots\alpha_L)$ can be written as $(\alpha_1\cdots\alpha_{L-s}\alpha^s_{L-s+1})$ for some $s \in \{1, 2, \ldots, L-1\}$, and where α_i^s means the sequence of s symbols α_i. A center cell is labeled by a sequence $(\alpha_1\alpha_2\cdots\alpha_{L-s}\alpha^{s-1}_{L-s+1}0)$. Its neighborhood set consists of 2^d cells, labeled by the sequences $(\alpha_1\alpha_2\cdots\alpha^{s-1}_{L-s+1}1)$, $(\alpha_1\alpha_2\cdots\alpha_{L-s}\alpha^{s-1}_{L-s+1}2)$, …, and $(\alpha_1\alpha_2\cdots\alpha_{L-s}\alpha^{s-1}_{L-s+1}2^d)$, respectively. A joint cell labeled by $(\alpha_1\cdots\alpha_{L-s}\alpha^s_{L-s+1})$, with $\alpha_{L-s+1} \neq 0$, has a neighborhood set with two elements. One is the center cell labeled by $(\alpha_1\cdots\alpha_{L-s}\alpha^{s-1}_{L-s+1}0)$. The other neighbor is another joint cell labeled by $(\alpha_1\cdots\alpha_{L-s-1}\alpha_{L-s+1}\beta^s)$, if $\alpha_{L-s} = 0$; or by $(\alpha_1\cdots\alpha_{L-s-1}0\beta^s)$, if $\alpha_{L-s} \neq 0$; where β is an allowed symbol that satisfies $\mathrm{mod}_{2^d+1}(\alpha_{L-s+1} + \beta) = 0$. This procedure identifies any two joint cells as reciprocal neighbors. On the other hand, an edge cell labeled by the sequence $(\alpha_1\cdots\alpha_{L-s}\alpha^s_{L-s+1})$ can not be assigned a reciprocal neighbor from the above procedure; thus this edge possesses only one neighbor, the center cell labeled by $(\alpha_1\cdots\alpha_{L-s}\alpha^{s-1}_{L-s+1}0)$. Because the symbols α_i belong to an enumeration system in base $(2^d + 1)$, a cell in the network labeled by the sequence $(\alpha_1\alpha_2\cdots\alpha_L)$ can be univocally associated to an integer index $i = 0, 1, 2, \ldots, (2^d + 1)^L - 1$, by the rule

$$(\alpha_1\alpha_2\cdots\alpha_L) \leftrightarrow i = \sum_{j=1}^{L} \alpha_j (2^d + 1)^{L-j}. \tag{1}$$

As an illustration, consider the fractal growth network embedded in an Euclidean space of dimension $d = 2$, as in Fig. 1(a). At the level of construction $L = 3$, the cell labeled by $(233) = (23^2)$ is a joint cell and has index $i = 68$, according to the rule Eq. (1). Its two neighbors, labeled by (230) (a center cell) and $(022) = (02^2)$ (another joint cell), are assigned indexes $i = 65$ and 12, respectively. Similarly, the cell $(422) = (42^2)$ is an edge with associated index $i = 112$; its only neighbor is the center cell (420), corresponding to $i = 110$.

3. Coupled map lattice model for pattern formation

A network might be considered as the spatial support of a dynamical spatiotemporal processes with either discrete or continuous-time. Here we consider reaction–diffusion and pattern formation phenomena on fractal growth networks. By associating a nonlinear function to each cell of a given fractal network and coupling these functions through nearest-neighbor diffusion interaction, we define a coupled map lattice that describes a reaction–diffusion dynamics as follows:

$$x_{t+1}(i) = f(x_t(i)) + \gamma \sum_{j\in\mathcal{N}(i)} (x_t(j) - x_t(i)), \tag{2}$$

where $x_t(i)$ represents the state of the cell having index i, assigned by Eq. (1), at discrete time t; $f(x_t(i))$ is a nonlinear function specifying the local dynamics; $\mathcal{N}(i)$ is the neighborhood set of the cell with index i; γ is a parameter expressing the coupling strength among neighboring cells and it plays the role of a homogeneous diffusion constant. The value of γ must be in an interval such that the local variables $x_t(i)$ in Eq. (2) are in the definition range for the local map $f(x_t(i))$. The form of the coupling term in Eq. (2) is usually called backward diffusive coupling and corresponds to a discrete version of the Laplacian in reaction–diffusion equations. This coupled map model can be generalized to include other coupling schemes, nonuniform coupling, or continuous-time local dynamics.

Eq. (2) can be written in a vector form as

$$\mathbf{x}_{t+1} = \mathbf{f}(\mathbf{x}_t) + \gamma \mathbf{M}\mathbf{x}_t. \tag{3}$$

The state vector $\mathbf{x}_t$ has N components $[\mathbf{x}_t]_i = x_t(i)$, $i = 0, \ldots, N-1$, corresponding to the states $x_t(i) = x_t(\alpha_1\alpha_2\cdots\alpha_L)$ of the cells on the network. The $N \times N$ real, symmetric matrix $\mathbf{M}$ expresses the coupling among the N components $x_t(i)$. For a fractal growth network embedded in an Euclidean space of dimension d at the level of construction L, the components of the corresponding matrix $\mathbf{M}$, denoted by $M(i, j)$ $(i, j = 0, 1, \ldots, N-1)$, are

$$M(i, j) = M(j, i) = \begin{cases} 1 & \text{if } j \in \mathcal{N}(i), \\ -|\mathcal{N}(i)| & \text{if } i = j, \\ 0 & \text{elsewhere}, \end{cases} \tag{4}$$

where $|\mathcal{N}(i)|$ is the cardinality of the neighborhood set $\mathcal{N}(i) = \mathcal{N}(\alpha_1\alpha_2\cdots\alpha_L)$. The matrix $\mathbf{M}$ plays the role of the spatially discrete diffusion operator on these networks, similar to the Laplacian in a spatially continuous reaction–diffusion equation.

4. Spectrum of the coupling matrix

The spatial patterns that can take place on fractal growth networks are determined by the eigenmodes of the coupling matrix $\mathbf{M}$, similarly to reaction–diffusion processes on regular Euclidean lattices [11,12]. On the other hand, the stability of the synchronized states is related to the set of eigenvalues of $\mathbf{M}$.

In order to analyze the eigenvector problem, consider a fractal growth network embedded in an Euclidean space of dimension d, at level of construction L, on which a spatiotemporal dynamics has been defined in the vector form of Eq.(3). The complete set of orthonormal eigenvectors of the corresponding matrix $\mathbf{M}$ can be described as the superposition of two distinct subsets of eigenmodes. One subset, which will be denoted by $\{\mathbf{u}_{mn}\}$, contains those eigenvectors associated to nondegenerate eigenvalues; and the other subset comprises the eigenvectors corresponding to degenerate eigenvalues of $\mathbf{M}$, and will be represented by $\{\mathbf{v}^g_{mn}\}$ (the indices refer to the degeneracy, as explained bellow). Thus, the complete set of eigenvectors of $\mathbf{M}$ is $\{\mathbf{u}_{mn}\} \cup \{\mathbf{v}^g_{ms}\}$. Each eigenvector describes a basic spatial pattern that may arise on a fractal growth network characterized by an embedding dimension d and a level of construction L. As illustration, we shall show the eigenvalues and eigenvectors of the coupling matrix corresponding to the fractal growth network embedded in the plane.

4.1. Nondegenerate eigenvectors

The eigenvectors of $\mathbf{M}$ belonging to the nondegenerate subset $\{\mathbf{u}_{mn}\}$ satisfy

$$\mathbf{M}\mathbf{u}_{mn} = b_{mn}\mathbf{u}_{mn}, \qquad \text{if } m = 0, n = 0, \quad \text{if } m = 1, 2, \ldots, L, n = 1, 2, \ldots, 3^{m-1}, \tag{5}$$

where b_{mn} is a eigenvalue associated to the eigenvector $\mathbf{u}_{mn}$. The i component of vector $\mathbf{u}_{mn}$ is $[\mathbf{u}_{mn}]_i = \mathbf{u}_{mn}(\alpha_1\alpha_2\cdots\alpha_L)$, according to the rule in Eq. (1). The number of eigenvectors in this subset and that of their corresponding eigenvalues, denoted by $\nu(b)$, is

$$\nu(b) = 1 + \sum_{m=1}^{L} 3^{m-1} = \frac{3^L + 1}{2}. \tag{6}$$

Any eigenvector $\mathbf{u}_{mn}$ in the nondegenerate subset $\{\mathbf{u}_{mn}\}$ is characterized by the following property: its components corresponding to cells of the same type on the network and located at the same distance (measured in number of

cells) from the center cell (0^L) are identical. Because of this property, we also refer to the elements in the subset $\{\mathbf{u}_{mn}\}$ as *symmetric* eigenvectors.

The index m corresponds to the level of construction at which the eigenvalue b_{mn} first appears, and it is related to the length of the longest diagonals that arise as the fractal growths up to the level L. At a level of construction $L > 1$ there is a total of $(2^d + 1)^{L-1} + 1$ diagonals on the network, which can be classified in L distinct families or groups according to their lengths, measured in terms of number of cells on the diagonal. Each different family of diagonals can be identified by the index $m = 1, 2, \ldots, L$, and each family contains all the diagonals of the network that have 3^m cells, and thus can support a wavelength of 3^m. The index m gives the step in the construction process at which the family of diagonals of length 3^m has first appeared. For a network defined at level L, there are $(2^d \times (2^d + 1)^{L-m-1})$ diagonals in each family characterized by $m = 1, 2, \ldots, L - 1$, and two diagonals in the family corresponding to $m = L$. For example, in Fig. 1(c) with $d = 2$ and $L = 3$, there are three families of diagonals according to their lengths: the family $m = 1$ contains 20 short diagonals with a length of three cells; the family $m = 2$ has four medium diagonals measuring nine cells; and the family $m = 3$ possesses two long diagonals with 27 cells. Additionally, we must count the family $m = 0$ associated to diagonals having one element; this corresponds to the spatially homogeneous eigenvector. Thus, the index $m = 0, 1, \ldots, L$, indicates the level of construction at which the family of diagonals characterized by the index m and having the same length of 3^m cells has appeared. The family of diagonals identified by m remains in the fractal as the network grows up to level L.

The index n counts the number of distinct symmetric eigenvectors that have originated each time a new family of diagonals of length 3^m cells appear, and it depends on the number of intersections that a new diagonal of length 3^m has with the other diagonals already present in the network. There is one intersection for each three cells in a diagonal; thus the number of intersections is 3^{m-1}. These intersections determine the different wavelengths that can be formed on a diagonal of length 3^m. The number of these different wavelengths having reflection symmetry about the long diagonal of length 3^m originated at step m can be counted by $n = 1, 2, \ldots, 3^{m-1}$.

The spatially homogeneous eigenvector of the matrix $\mathbf{M}$, which we denote by $\mathbf{u}_{00}$, belongs to the subset $\{\mathbf{u}_{mn}\}$ and its components N are

$$\mathbf{u}_{00}(\alpha_1 \cdots \alpha_L) = N^{-1/2}; \qquad \forall L, \quad \forall \alpha_k \tag{7}$$

and

$$\mathbf{u}_{00} = \frac{1}{\sqrt{N}}\mathrm{col}(1, 1, \ldots, 1). \tag{8}$$

Since the eigenvectors of $\mathbf{M}$ are mutually orthogonal, all others eigenmodes in either subset $\{\mathbf{u}_{mn}\}$ or $\{\mathbf{v}^g_{mn}\}$ must satisfy

$$\sum_{\alpha_1,\ldots,\alpha_L} \mathbf{u}_{mn}(\alpha_1 \cdots \alpha_L) = 0; \quad \forall \alpha_k, \quad m \neq 0; \qquad \sum_{\alpha_1,\ldots,\alpha_L} \mathbf{v}^g_{mn}(\alpha_1 \cdots \alpha_L) = 0; \quad \forall \alpha_k, \tag{9}$$

that is, the sum over the components of any eigenvector of $\mathbf{M}$, different of $\mathbf{u}_{00}$, is zero.

Fig. 2(a) shows the $\nu(b) = 5$ nondegenerate eigenvectors and their associated eigenvalues of the coupling matrix corresponding to a fractal growth network embedded in dimension $d = 2$ and having a level of construction $L = 2$. Fig. 2(b) shows the subset of degenerate eigenvectors $\mathbf{v}^g_{ms}$ and the eigenvalues corresponding to a fractal growth network embedded in an Euclidean space of dimension $d = 2$, at level of construction $L = 2$.

The set of eigenvalues arising from Eq. (5) may be ordered by decreasing value. By Gershgorin's theorem [13], the homogeneous eigenvector possesses the largest eigenvalue of $\mathbf{M}$, which is $b_{00} = 0$. In the case of embedding dimension $d = 2$, the smallest eigenvalue for large L is found to be

$$\lim_{L\to\infty} b_{L\,3^{L-1}} = -(4 + \sqrt{2}). \tag{10}$$

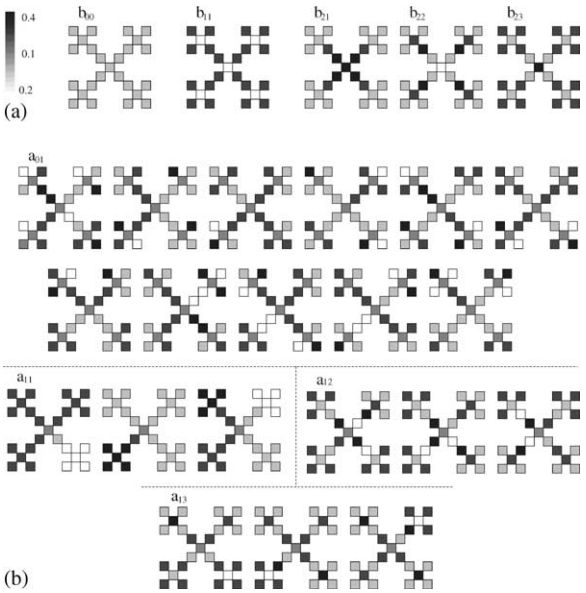

Fig. 2. Fractal growth network corresponding to embedding dimension $d = 2$ and level of construction $L = 2$. (a) The five nondegenerated, symmetric eigenvectors $\mathbf{u}_{mn}$ and their corresponding eigenvalues. (b) Degenerate eigenvectors $\mathbf{v}_{mn}$ and their corresponding eigenvalues.

For each index $m > 1$, the eigenvalues $\{b_{m1}, b_{m2}, \ldots, b_{m3^{m-1}}\}$ arise in groups of three, b_{mn}, $b_{mn'}$ and $b_{mn''}$, where

$$n' = 2 \times 3^{m-1} - n + 1; \qquad n'' = 2 \times 3^{m-1} + n. \tag{11}$$

The sum of the eigenvalues in each of these groups is constant, and gives

$$b_{mn} + b_{mn'} + b_{mn''} = -(2^d + 4). \tag{12}$$

Because of (12), the eigenvalues associated to the nondegenerate eigenvectors satisfy

$$\sum_{m=0}^{L} \sum_{n=0}^{3^{m-1}} b_{mn} = -(2^d + 4) \sum_{m=1}^{L} 3^{m-1} = -(2^{d-1} + 2)(3^L - 1). \tag{13}$$

Fig. 3 shows the spectrum of eigenvalues $\{b_{mn}\}$, indicated by empty symbols, for a fractal growth network embedded in an Euclidean space of dimension $d = 2$, at successive construction levels L. Eigenvalues associated to degenerate eigenvectors of the coupling matrix $\mathbf{M}$, to be discussed next, are also shown in Fig. 3.

4.2. Degenerated eigenvectors

The subset of degenerate eigenvectors $\{\mathbf{v}^g_{mn}\}$ of the matrix $\mathbf{M}$ satisfy

$$\mathbf{M}\mathbf{v}^g_{mn} = a_{mn}\mathbf{v}^g_{mn}, \qquad m = 1, 2, \ldots, L; \quad n = 1, 2, \ldots, 3^{m-1}, \tag{14}$$

where a_{mn} is the eigenvalue associated to a group of Ω degenerate eigenvectors $\{\mathbf{v}^1_{mn}, \mathbf{v}^2_{mn}, \ldots, \mathbf{v}^{\Omega}_{mn}\}$ belonging to the subset $\{\mathbf{v}^g_{mn}\}$. The index g runs from 1 to a value Ω and counts the different eigenvectors associated to the degenerate eigenvalue a_{mn}, as it will be shown bellow. The integer indices m and n label different eigenvalues a_{mn}.

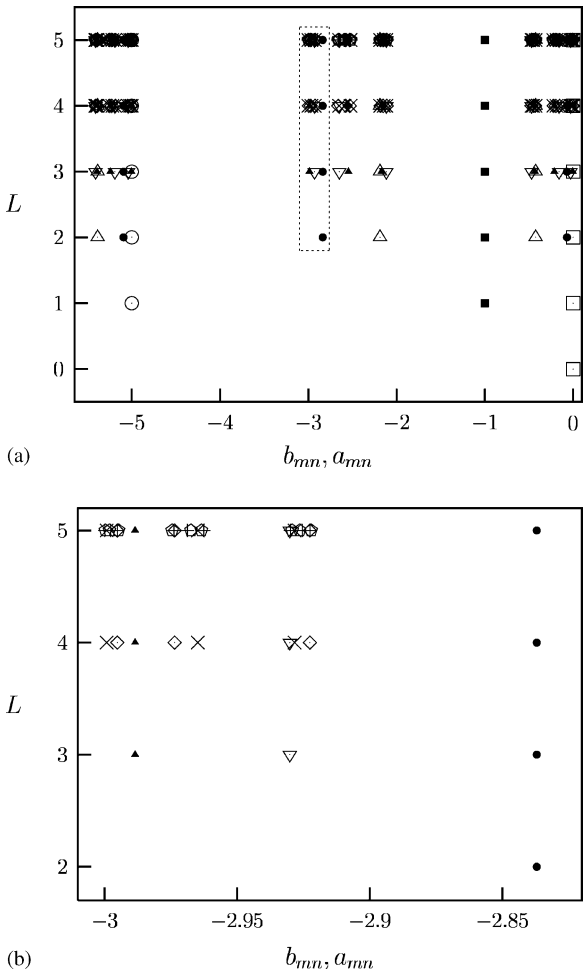

Fig. 3. Spectrum of eigenvalues of the coupling matrix at increasing construction levels L, for a fractal growth network embedded in dimension $d = 2$. (a) Eigenvalues b_{mn} are indicated by empty symbols: b_{00} (□); b_{11} (⊙); b_{2n} (△); b_{3n} (∇); b_{4n} (◇). Other symbols indicate eigenvalues a_{mn} as follows: a_{1n} (■); a_{2n} (●); a_{3n} (▲); a_{4n} (×); a_{5n} (+). (b) Magnification of the dotted region in (a).

The i-component of a vector $\mathbf{v}^g_{mn}$ corresponds to a cell of the network labeled by the rule Eq. (1), i.e., $[\mathbf{v}^g_{mn}]_i = \mathbf{v}^g_{mn}(\alpha_1\alpha_2\cdots\alpha_L)$. The eigenmodes in the subset $\{\mathbf{v}^g_{mn}\}$ are characterized by the following two properties:

$$\mathbf{v}^g_{mn}(\alpha_1\cdots\alpha_{L-m}0^m) = 0; \qquad m = 1, 2, \ldots, L-1, \tag{15}$$

that is, all the components of $\mathbf{v}^g_{mn}$ corresponding to center cells formed in the first $L - m$ levels of construction vanish

$$\sum_{\alpha_1,\alpha_2,\ldots,\alpha_{L-1}} \mathbf{v}^g_{mn}(\alpha_1\alpha_2\cdots\alpha_{L-1}0) = 0; \tag{16}$$

that is, the sum of the components associated to the center cells in a network spatially described by a vector $\mathbf{v}^g_{ms}$, is zero.

In contrast to the eigenvectors in the nondegenerate subset, an eigenvector $\mathbf{v}^g_{ms}$ is nonsymmetric; however it exhibits a partial regularity, having all its components corresponding to center cells equal to zero if they originated

at the level of construction $L-m$. The index m counts the number of additional levels of construction in which nonvanishing center cells have appear up to level L; and its possible values are $m=1,2,\ldots,L$. There are $(2^d+1)^{L-m}$ vanishing center cells in an eigenvector $\mathbf{v}_{ms}^g$. Each null center cell in the eigenvector is the center of $2^{d-1}-1$ diagonals, except the cell (0^L) that is the center of one additional diagonal. Thus, adding the additional diagonal of the center cell (0^L), there are $(2^d+1)^{L-m}(2^{d-1}-1)+1$ diagonals whose centers are null center cells. The index n counts the number of possible intersections that these diagonals have with other diagonals; its possible values are $n=1,2,\ldots,3^{m-1}$.

Because an eigenvector $\mathbf{v}_{ms}^g$ is a nonsymmetric mode, the two edge cells at the ends of each of the $(2^d+1)^{L-m}(2^{d-1}-1)+1$ diagonals having null center cells are independent of each other. Therefore, there exist $2[(2^d+1)^{L-m}(2^{d-1}-1)+1]$ edge cells with this characteristics, for given values of m and n. However, due to the orthogonality property, Eq. (9), the total number of linearly independent eigenvectors $\mathbf{v}_{ms}^g$ possessing the same indices m and n is $\Omega=2[(2^d+1)^{L-m}(2^{d-1}-1)+1]-1$. The index g counts the number of independent eigenvectors associated to an eigenvalue a_{mn}, and it may take the values $g=1,2,\ldots,\Omega$. In this fashion, the subset of degenerate eigenvectors $\{\mathbf{v}_{ms}^g\}$ of the coupling matrix $\mathbf{M}$ corresponding to a fractal growth network embedded in dimension d and at level of construction L is fully described.

In the case of embedding dimension $d=2$, there are 5^{L-m} vanishing center cells in an eigenvector $\mathbf{v}_{ms}^g$ and there are $5^{L-m}+1$ diagonals whose centers are null center cells. The number of linearly independent eigenvectors $\mathbf{v}_{ms}^g$ having the same indices m and n is $\Omega=2(5^{L-m}+1)-1=2\times 5^{L-m}+1$. Thus, the index g may take the values $g=2,\ldots,2\times 5^{L-m}+1$.

The number of different eigenvalues, a_{mn}, that belong to the spectrum of matrix $\mathbf{M}$ for a fractal growth network at construction level L, is

$$\nu(a)=\sum_{m=1}^{L}3^{m-1}=\frac{3^L-1}{2}. \tag{17}$$

At each level $m>1$, there appear 3^{m-1} new eigenvalues a_{mn}. Similarly to the nondegenerate eigenvalues, the a_{mn} can be grouped in sets of three eigenvalues that satisfy

$$a_{mn}+a_{mn'}+a_{mn''}=-(2^d+4), \tag{18}$$

where

$$n'=2\times 3^{m-1}-n+1, \qquad n''=2\times 3^{m-1}+n, \tag{19}$$

and therefore the total sum of the degenerate eigenvalues a_{mn} of a matrix $\mathbf{M}$ corresponding to a fractal growth network embedded in a dimension d and at level of construction L gives

$$\sum_{m=1}^{L}\sum_{n=1}^{3^{m-1}}a_{mn}=-(2^d+4)\sum_{m=1}^{L}3^{m-1}=-(2^{d-1}+2)(3^{L-1}-1). \tag{20}$$

Fig. 3 shows the spectrum of eigenvalues $\{a_{mn}\}\cup\{b_{mn}\}$ for a fractal growth network embedded in Euclidean space of dimension $d=2$ at successive levels of construction L. The distribution of the spectrum of eigenvalues of the coupling matrix $\mathbf{M}$ can be seen as a function of the growth process of the fractal structure. Note that the full spectrum $\{a_{mn}\}\cup\{b_{mn}\}$ is always contained between the eigenvalues $b_{00}=0$ and $b_{L3^{L-1}}$.

From Eqs. (6) and (17), the total number of distinct eigenvalues of $\mathbf{M}$, including both types a_{mn} and b_{mn}, and denoted by $\nu(\mathbf{M})$ is given by

$$\nu(\mathbf{M})=\nu(b)+\nu(a)=\tfrac{1}{2}(3^L+1)+\tfrac{1}{2}(3^L-1)=3^L. \tag{21}$$

Since there appear 3^{m-1} new eigenvalues of type a_{mn} at each level of construction m, and there are $\Omega=2[(2^d+1)^{L-m}(2^{d-1}-1)+1]-1$ eigenvectors $\mathbf{v}_{ms}^g$ associated to each eigenvalue a_{mn}, the total number of independent

eigenvectors in the subset $\{\mathbf{v}^g_{mn}\}$ is

$$\sum_{m=1}^{L} \Omega(3^{m-1}) = (2^d+1)^L - \frac{3^L+1}{2}. \tag{22}$$

From Eq. (6) we know that the number of independent eigenvectors in the subset $\{\mathbf{u}_{mn}\}$ is $(3^L+1)/2$. Therefore, the total number of independent eigenvectors of $\mathbf{M}$ is

$$\tfrac{1}{2}(3^L+1) + (2^d+1)^L - \tfrac{1}{2}(3^L+1) = (2^d+1)^L = N, \tag{23}$$

as should be expected.

Fig. 4(a) shows the complete spectrum of eigenvalues of $\mathbf{M}$ and the degeneracy fraction of each eigenvalue, for a fractal growth network embedded in an Euclidean space of dimension $d=2$, at level of construction $L=5$. The degeneracy $\Omega = 2\times 5^{5-m}+1$ of each of the $\nu(a) = (3^5-1)/2 = 121$ eigenvalues a_{mn} is plotted as a vertical bar, while the $\nu(b) = (3^5+1)/2 = 122$ different eigenvalues b_{mn} are indicated by plus symbols (+) and they are nondegenerate. It is clear that both the distribution of eigenvalues and their degeneracies are nonuniform. The scaling properties of the spectrum of eigenvalues of the coupling matrix can also be conveniently represented by plotting the accumulated sum of the degeneracies of all eigenvalues, that is, the measure of the spectrum of $\mathbf{M}$ (denoted by ρ), on the eigenvalue axis for large L, as in Fig. 4(b). The resulting graph exhibits the features of a devil staircase, a fractal curve arising in a variety of nonlinear phenomena.

The eigenvectors of the coupling matrix reflect the topology of the fractal growth network and they are analogous to the Fourier eigenmodes appearing in regular Euclidean lattices. In this sense, the symmetry properties of the nondegenerate eigenvectors $\{\mathbf{u}_{mn}\}$ and the conditions given in Eqs. (15) and (16) for the degenerate eigenvectors $\{\mathbf{v}^g_{ms}\}$ represent different wavelengths on a fractal growth network embedded in an Euclidean space of dimension d at level of construction L.

5. Synchronized states and pattern selection

Synchronized states in spatiotemporal systems are relevant since we are often interested in mechanisms by which a spatial pattern can be selected in a uniform system that breaks its symmetry as a parameter is changed.

Consider spatially synchronized, period-K states such as $x_t(\alpha_1\cdots\alpha_L) = \bar{x}_k$, $\forall(\alpha_1\cdots\alpha_l)$; where $\bar{x}_k$, $(k = 1, 2, \ldots, K)$, is a period-K orbit of the local map, satisfying $f^{(K)}(\bar{x}_k) = \bar{x}_k$. The linear stability analysis of periodic, synchronized states in coupled map lattices is carried out by the diagonalization of the matrix $\mathbf{M}$ in Eq. (3), and it leads to the conditions [11]

$$\prod_{k=1}^{K} |f'(\bar{x}_k) + \gamma\mu| < 1, \tag{24}$$

where μ is any of the $\nu(\mathbf{M}) = 3^L$ eigenvalues, associated to either subset of eigenvectors $\{\mathbf{u}_{mn}\}$ or $\{\mathbf{v}^g_{ms}\}$, of the coupling matrix $\mathbf{M}$ corresponding to a fractal growth network embedded in a d-dimensional Euclidean space at level of construction L.

The nonuniform distribution of the eigenvalue spectrum is manifested in the stability of the synchronized states through Eq. (24) and gives rise to marked differences when compared, for instance, with the bifurcation structure on regular lattices. As an application, consider a local dynamics described by the logistic map, $f(x) = \lambda x(1-x)$. In this case, the stability conditions, Eq. (24), for the period $K = 2^p$, synchronized state yield the set of boundary

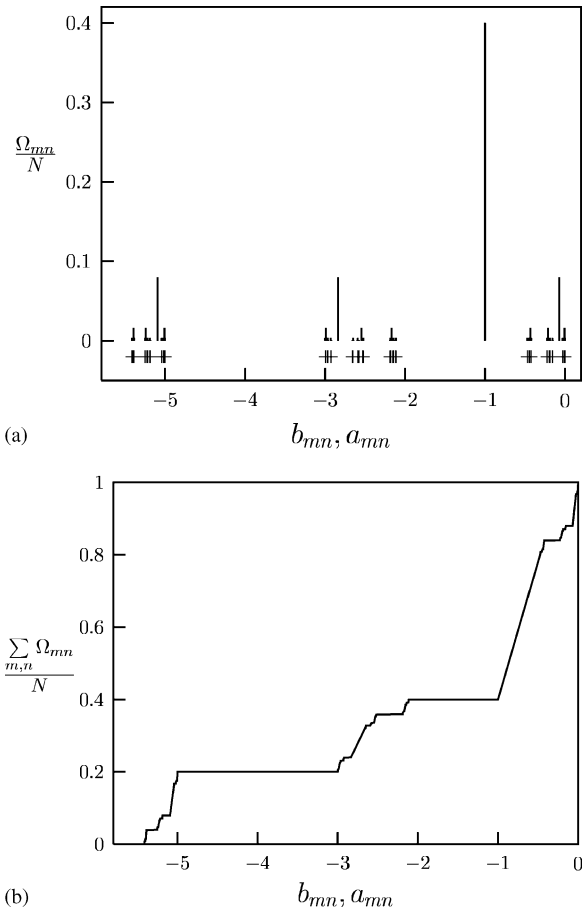

Fig. 4. (a) Distribution and degeneracies of the spectrum of eigenvalues of the coupling matrix **M** for a fractal growth network embedded in $d = 2$ at level of construction $L = 5$. The eigenvalues b_{mn} are indicated with (+) just below the zero line, for clarity. The vertical axis shows the degeneracy of the eigenvalues $\{a_{mn}\}$ divided by N, indicated by a vertical bar at each eigenvalue. (b) The measure of the full set of eigenvalues of **M**.

curves

$$S_L^p(\mu) \equiv \prod_{k=1}^{2^p} [\lambda(1 - 2\bar{x}_k) + \gamma\mu] = \pm 1. \tag{25}$$

For each sign, Eq. (25) give 3^L boundary curves in the plane (γ, λ), corresponding to the different values of μ; these curves determine the stability regions of the period-2^p, synchronized states on the network.

The scaling structure for the period-2^p, synchronized states in fractal growth networks is similar to that of a any lattice described by a diffusive coupling matrix, since the form of Eq. (25) is the same in any case. As for regular Euclidean lattices [11,12], the stability regions for the period-2^p, synchronized states in the (γ, λ) plane scale as $\lambda \sim \delta^{-p}$, and $\gamma \sim \alpha^{-p}$, where $\delta = 4.669\ldots$ and $\alpha = -2.502\ldots$ are Feigenbaum's scaling constants for the period doubling transition to chaos. However, the specific structure of the eigenvalue spectrum of the coupling matrix determines the shapes and gaps of the regions of stability of synchronized, periodic states.

From Eq. (25), the boundary curves for the synchronized, fixed point state ($p = 0$) on the parameter plane (γ, λ) are given by the straight lines

$$\lambda = \mu\gamma + 1, \qquad \lambda = \mu\gamma + 3, \tag{26}$$

which are first crossed for the most negative eigenvalue, $\mu = b_{L3^{L-1}}$. Similarly, the boundaries period-two ($p = 1$), synchronized state on a fractal growth network embedded in an Euclidean space of dimension $d = 2$ and at construction level $L = 3$ are given by the two sets

$$S_3^1(a_{mn}) = -\lambda^2 + 2\lambda + 4 + \gamma a_{mn}(\gamma a_{mn} - 2) = \pm 1, \tag{27}$$

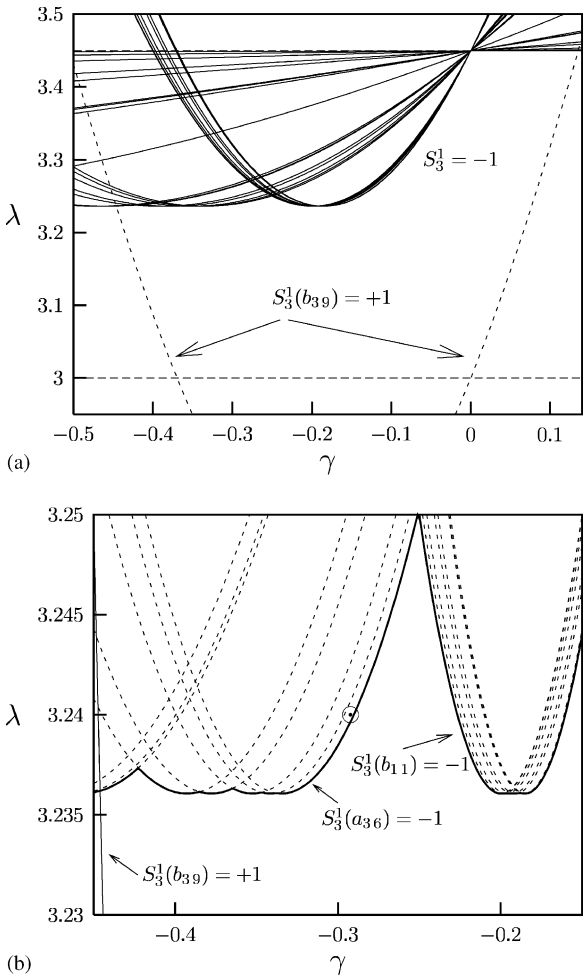

Fig. 5. The boundary curves $S_3^1 = \pm 1$ given by Eqs. (27) and (28) for the period-two, synchronized states of a fractal growth network at level of construction $L = 3$, embedded in $d = 2$. (a) The upper curves correspond to the r.h.s. of Eqs. (27) and (28) equal to -1 for both types of eigenvalues. Arrows indicate the boundary curve $S_3^1(b_{39}) = +1$. The interior region bounded by these curves is where stable, synchronized, period-two states exist in the parameter plane (λ, γ). (b) Magnification of the upper curves in (a), showing the gaps in the stability boundaries of the period-two, synchronized states. Arrows indicate boundary curves corresponding to several eigenvalues. The symbol ($\odot$) just beyond the boundary $S_3^1(b_{36}) = -1$ indicates the values of the parameters γ and λ used in Fig. 6.

and

$$S_3^1(b_{mn}) = -\lambda^2 + 2\lambda + 4 + \gamma b_{mn}(\gamma b_{mn} - 2) = \pm 1. \tag{28}$$

Fig. 5(a) shows the boundary curves Eqs. (27) and (28) on the plane (γ, λ). The boundary between the synchronized, fixed point state and the synchronized period-two state occurs at $\lambda = 3$. The upper boundaries (corresponding to -1 in the r.h.s. of Eqs. (27) and (28)) have minima $\lambda_{\min} = 1 + \sqrt{5}$ at values $\gamma_{\min} = 1/b_{mn}$ and $\gamma_{\min} = 1/a_{mn}$ (for any period-2^p, $\lambda_{\min}$ depends on p). Fig. 5(b) shows a magnification of Fig. 5(a) around the minima of the upper boundaries. The distribution of the minima $\gamma_{\min}$ and the presence of nonuniformly distributed gaps in the boundary curves is a manifestation of the nonuniform structure of the eigenvalue spectrum. Since the nonuniformity in the distribution of eigenvalues persists at any construction level L of a fractal growth network, this property allows for regions of stability of the synchronized states or gaps characteristic of fractal networks and which are not present in other geometries, for example in regular lattices, where the distribution of eigenvalues of the coupling matrix is uniform and continuous in the limit of infinite size lattices.

The set of eigenvectors $\{\mathbf{u}_{mn}\} \cup \{\mathbf{v}_{mn}^g\}$ of the coupling matrix $\mathbf{M}$ constitute a complete basis (normal modes) on which a state $\mathbf{x}_t$ of the system can be represented as a linear combination of these vectors. Thus the evolution of $\mathbf{x}_t$ reflects the stabilities of the normal modes. Fig. 5(b) shows how a spatially inhomogeneous pattern may be selected as the synchronized state becomes unstable through crossing of the upper boundary; the first boundary segment crossed determines the character of the instability and the properties of the selected pattern. For example, consider an initial state consisting of a small perturbation of the synchronized, period-2 state at parameter values just beyond the boundary segment corresponding to the eigenvalue a_{36}, indicated by a cross in Fig. 5(b), where this initial state is unstable. The inhomogeneous period-four final spatial pattern is represented in Fig. 6; it corresponds to a linear combination of the three eigenmodes $\{\mathbf{v}_{36}^g; g = 1, 2, 3\}$ associated to the degenerate eigenvalue a_{36} of the matrix $\mathbf{M}$ corresponding to the fractal network embedded in dimension $d = 2$ at level of construction $L = 3$. All other modes are unstable in this region of parameter space. For any construction level L of the fractal network, and any period-2^p, the boundary curve $S_3^1(a_{36}) = -1$ separates a gap of the synchronized state from the stable region for

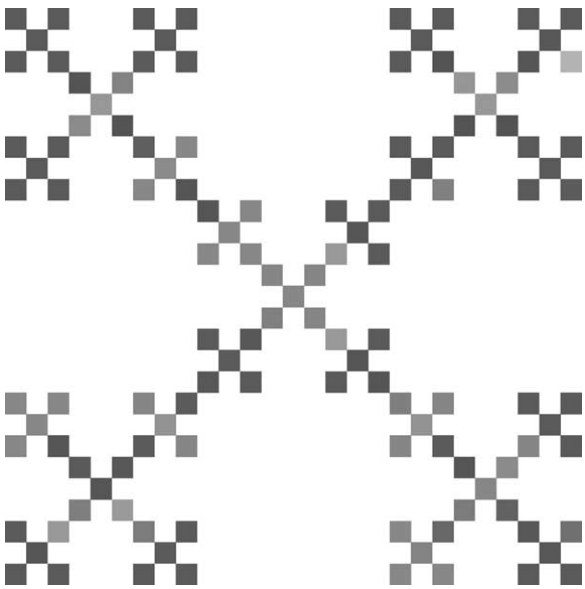

Fig. 6. Inhomogeneous, period-four state at parameter values $\gamma = -0.296$, $\lambda = 3.24$. This pattern is a linear combination of the three eigenvectors associated to the eigenvalue a_{36}.

the eigenmodes $\mathbf{v}_{36}^{g}$ corresponding to a_{36}. Therefore, a transition between these two spatial patterns can always be observed in the appropriate regions of the parameter plane (γ, λ).

6. Conclusions

The underlying inhomogeneous structure of fractal growth networks has significant effects on the spatial patterns that can be formed by reaction–diffusion processes on these geometrical supports. In systems of interacting elements, such as the models considered in this article, the coupling matrix contains the connectivity of the network. The set of eigenvectors of the coupling matrix reflect this connectivity. The spatial patterns that can arise in fractal growth networks are determined by the eigenvectors of the diffusion coupling matrix **M**, which constitute a complete basis on which any spatial mode can be expressed as a linear combination. These eigenvectors have complex spatial forms but they are analogous to the Fourier eigenmodes arising in regular Euclidean lattices. On the other hand, the stability of the synchronized states is determined by the eigenvalues of **M**. The density distribution of these eigenvalues and their degeneracy are nonuniform. These features affect the bifurcation properties of dynamical systems such as coupled maps defined on fractal growth networks. The scaling structure of the synchronized, period-doubled states on the space of parameters of the system is similar for both uniform and fractal networks but the nature of the bifurcation boundaries is different. For fractal growth networks, the nonuniform distribution of eigenvalues leads to gaps in the boundary curves separating stable synchronized states that are not present for coupled maps on uniform lattices, where the spectrum of eigenvalues is continuous. These gaps allow for the selection of specific spatial patterns arising from a uniform, synchronized state by appropriately changing the parameters of the system.

Although we have presented only the simplest spatiotemporal patterns that can be formed on fractal growth structures, the formalism introduced in this article can be applied to many other processes, such as excitable dynamics, nontrivial collective behavior, phase-ordering, domain segregation, turbulence, etc. The formalism is also useful for cellular automata models and continuous-time local dynamics on fractal growth networks.

The study of dynamical systems defined on nonuniform spatial supports, such as fractal growth networks, provides insight into the relationship between topology and spatiotemporal phenomena in complex networks.

Acknowledgement

This work was supported in part by Consejo de Desarrollo Científico, Humanístico y Tecnológico, Universidad de Los Andes, Mérida, Venezuela.

References

[1] K. Kaneko (Ed.), Chaos 2 (1992) 279, Focus issue on Coupled Map Lattices.
[2] M.G. Cosenza, R. Kapral, Phys. Rev. A (1992) 1850.
[3] K. Tucci, M.G. Cosenza, O. Alvarez-Llamoza, Phys. Rev. E 68 (2003) 027202.
[4] P.M. Gade, H.A. Cerdeira, R. Ramaswamy, Phys. Rev. E 52 (1995) 2478.
[5] M.G. Cosenza, K. Tucci, Phys. Rev. E 64 (2001) 026208.
[6] D. Volchenkov, S. Sequeira, Ph. Blanchard, M.G. Cosenza, Stochast. Dynam. 2 (2002) 203.
[7] M.G. Cosenza, K. Tucci, Phys. Rev. E 65 (2002) 036223.
[8] S. Jalan, R.E. Amritkar, Phys. Rev. Lett. 90 (2003) 014101.
[9] T. Vicsek, J. Phys. A: Math. Gen. 16 (1983) L647.
[10] T. Vicsek, Fractal Growth Phenomena, World Scientific, Singapore, 1989.
[11] I. Waller, R. Kapral, Phys. Rev. A 30 (1984) 2047.
[12] R. Kapral, Phys. Rev. A 31 (1985) 3868.
[13] S. Barnett, Matrices, Methods and Applications, Oxford University Press, Oxford, 1990.